

1 **Supplementary Information for**

2 **Revealing the Effect of Conductive Carbon Materials on the Sodium Storage**

3 **Performance of Sodium Iron Sulfate**

4 Wenqing Zhu,<sup>+a, b</sup> Zhiqiang Hao,<sup>+b, c</sup> Xiaoyan Shi,<sup>b</sup> Xunzhu Zhou,<sup>b, c</sup> Zhuo Yang,<sup>b, c</sup>

5 Lingling Zhang,<sup>b</sup> Zongcheng Miao,<sup>\* a</sup> Lin Li,<sup>\*b, c</sup> and Shu-Lei Chou<sup>\* b, c</sup>

6 a. School of Chemical and Environmental Engineering, Anhui Polytechnic

7 University, Wuhu, Anhui 241000, China. E-mail: miao宗cheng@ahpu.edu.cn

8 b. Institute for Carbon Neutralization, College of Chemistry and Materials

9 Engineering, Wenzhou University, Wenzhou, Zhejiang 325035, China. E-mail:

10 linli@wzu.edu.cn; chou@wzu.edu.cn

11 c. Wenzhou Key Laboratory of Sodium-Ion Batteries, Wenzhou University

12 Technology Innovation Institute for Carbon Neutralization, Wenzhou, Zhejiang

13 325035, China.

14 + These authors contributed equally to this work.

15

## 1 Experimental section

### 2 Synthesis of $\text{Na}_2\text{Fe}_2(\text{SO}_4)_3@\text{C}$

3  $\text{FeSO}_4 \cdot \text{H}_2\text{O}$  (Aladdin, 99.0%) was first annealed at 280 °C for 12 hours in an  $\text{N}_2$   
4 atmosphere to obtain anhydrous  $\text{FeSO}_4$ . The  $\text{Na}_2\text{Fe}_2(\text{SO}_4)_3@\text{C}$  (NFS@C) composites  
5 were synthesized through a low-temperature solid-state reaction method. Initially, a  
6 mixture was prepared by anhydrous  $\text{Na}_2\text{SO}_4$  (Aladdin, 99.0%) and anhydrous  $\text{FeSO}_4$  in  
7 a 1:2 molar ratio, along with different conductive carbons in a 7:1 mass ratio, such as  
8 Ketjen Black (Lion Corporation, EC-600JD), super p (Imerys, SUPER P-Li), acetylene  
9 black (Guangdong Canrd New Energy Technology Co., Ltd. Kappa 100), and  
10 conductive graphite KS6 (Imerys, KS-6). Finally, the mixture was homogeneously  
11 blended in a planetary ball mill under argon atmosphere at 800 rpm for 6 hours. Next,  
12 the precursor was transferred to a quartz tube filled with  $\text{N}_2$  atmosphere and subjected  
13 to a sintering process at 350 °C for 24 h. Finally, these particles were ground in a mortar  
14 and pestle for 10 min to obtain the final sample NFS@C. The samples were labeled as  
15 NFS@KB, NFS@SP, NFS@AB, and NFS@G, according to the type of conductive  
16 carbon used.

### 17 Material characterization

18 The crystal structure of the NFS@C composites was examined using an Aeris  
19 Research Benchtop X-Ray Diffractometer from Malvern Panalytical equipped with a  
20  $\text{CuK}\alpha$  radiation source. The morphologies of the composites were characterized by field  
21 transmission scanning electron microscopy (FE-SEM, EVO 10) and transmission

1 electron microscope (TEM, JEM-2100F). The specific surface area of  
2  $\text{Na}_2\text{Fe}_2(\text{SO}_4)_3@\text{C}$  composite material was investigated using a nitrogen adsorption and  
3 desorption analysis with a surface area and pore size analyzer (V-Sorb 2802TP). Raman  
4 spectra (HORIBA XploRA PLUS) were collected in the range of  $500\text{-}2500\text{ cm}^{-1}$  to  
5 characterize the carbon coating. The vibrational states of existing functional groups  
6 were examined via FT-IR (spectral resolution of  $4\text{ cm}^{-1}$  on a SHIMADZU IRAffinity-  
7 1S). Thermogravimetric (TG) analysis was conducted using an Integrated Thermal  
8 Analyzer (ZCT-A), at a heating rate of  $5\text{ }^\circ\text{C min}^{-1}$ , from room temperature to  $600\text{ }^\circ\text{C}$ .  
9 X-ray photoelectron spectroscopy (XPS, PHI-5000 VPIII) was utilized to investigate  
10 the chemical states of Fe and C elements.

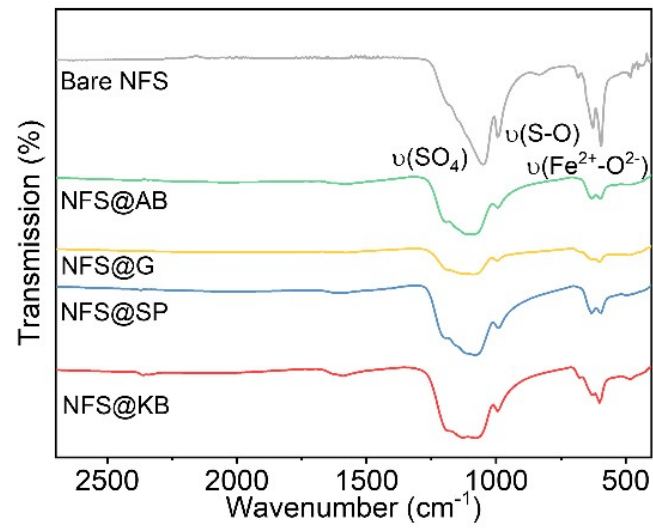
#### 11 Electrochemical characterization

12 The electrochemical properties of the  $\text{NFS}@\text{C}$  composites were performed in  
13 CR2032 coin half cells. The material powder was mixed with Ketjen Black and  
14 polyvinylidene fluoride (PVDF) binder (80:10:10 by weight) in N-methyl-2-  
15 pyrrolidone (NMP), and then the slurry was coated on an Al foil uniformly. The foil  
16 with active material was dried at  $80\text{ }^\circ\text{C}$  for 6 h in vacuum with a loading about  $1.5\text{-}2$   
17  $\text{mg cm}^{-2}$  and cut into circle electrode (diameter 10 mm). Sodium (Na) metal served as  
18 both the counter and reference electrode, while Glass fiber membranes (Whatman,  
19 GF/D) were utilized as separators. The electrolyte adopted was 1 M  $\text{NaClO}_4$  in a  
20 mixture of EC/DEC (1:1 in volume) with an additional 2 wt% FEC. Concerning the  
21 fabrication of graphite electrode for the assembly of full cells, an 80% mixture of

1 Japanese carbon was combined with 10% super p and 10% Water-based adhesive (SA2)  
2 binder, subsequently applied as a coating on Al foil, and utilized as the anode in the  
3 coin cell architecture. All the coin cells were assembled inside a glove box filled with  
4 Ar gas, wherein the levels of O<sub>2</sub> and H<sub>2</sub>O were meticulously regulated to remain below  
5 0.1 ppm. Galvanostatic charge/discharge tests were conducted on a Neware test system  
6 (Neware Technology Limited) under various current densities. The voltage window  
7 between 2 and 4.5 V was selected. In addition, Cyclic Voltammetry (CV) tests were  
8 conducted on the CHI660E electrochemistry workstation with scan speeds ranging  
9 from 0.1 to 0.5 mV s<sup>-1</sup>.

10

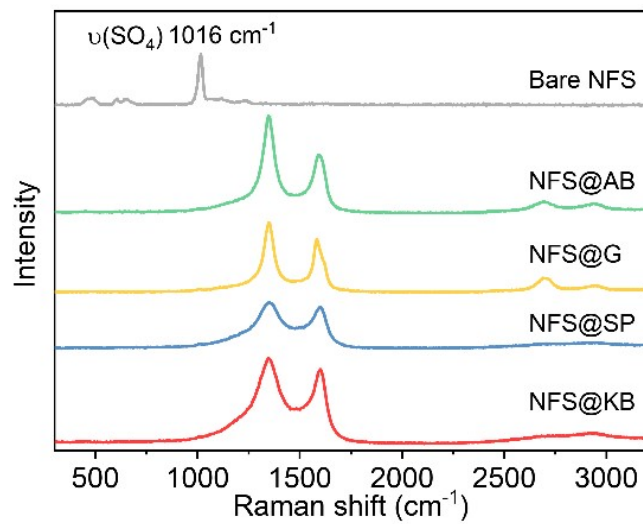
1



2

3 **Figure S1.** FT-infrared spectra of NFS@C composite materials and bare NFS.

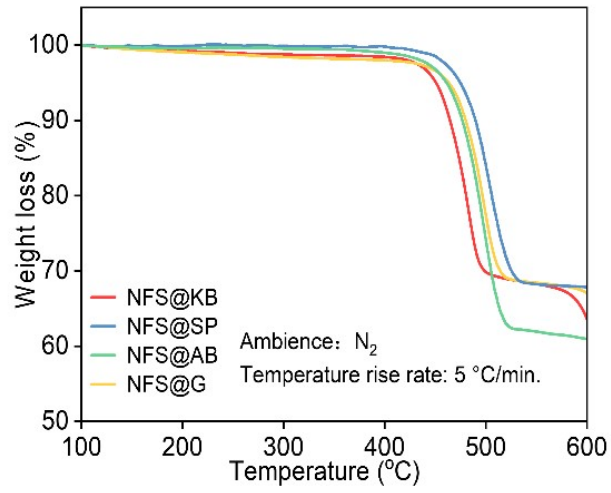
4



1

2 **Figure S2.** Raman spectrum of NFS@C composite materials and bare NFS.

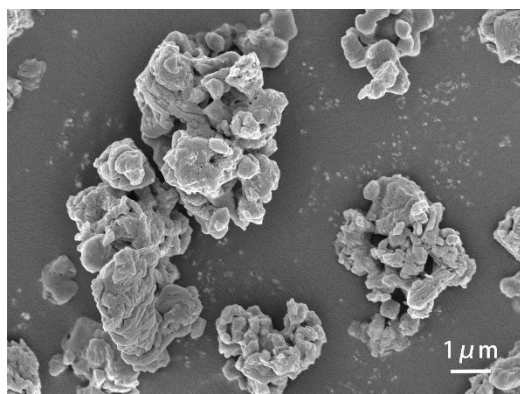
3



1

2 **Figure S3.** TG curve of NFS@C composite materials in N<sub>2</sub> atmosphere.

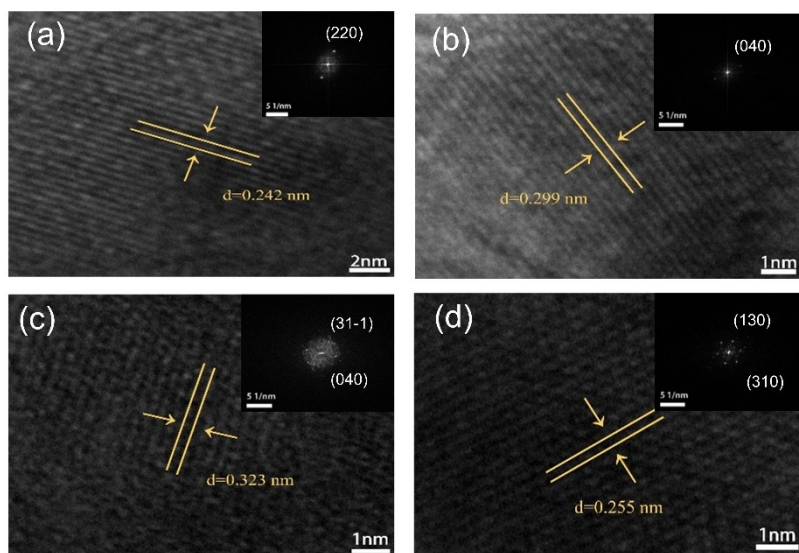
3



1

2 **Figure S4.** SEM image of bare NFS.

3

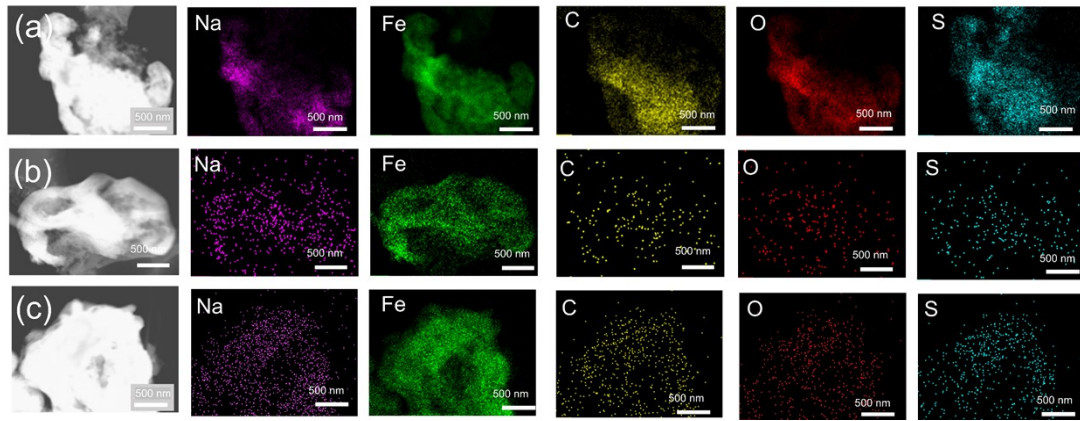


1

2 **Figure S5.** Enlarged lattice fringes of (a) NFS@KB, (b) NFS@SP, (c) NFS@AB, and

3 (d) NFS@G, and the FFT image in the inset.

4

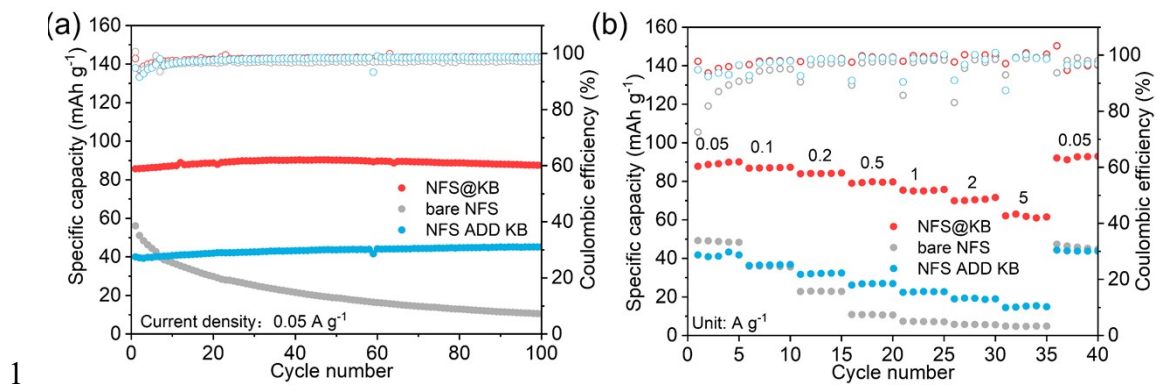


1

2 **Figure S6.** HAADF image and the corresponding Na, Fe, C, O, and S elemental

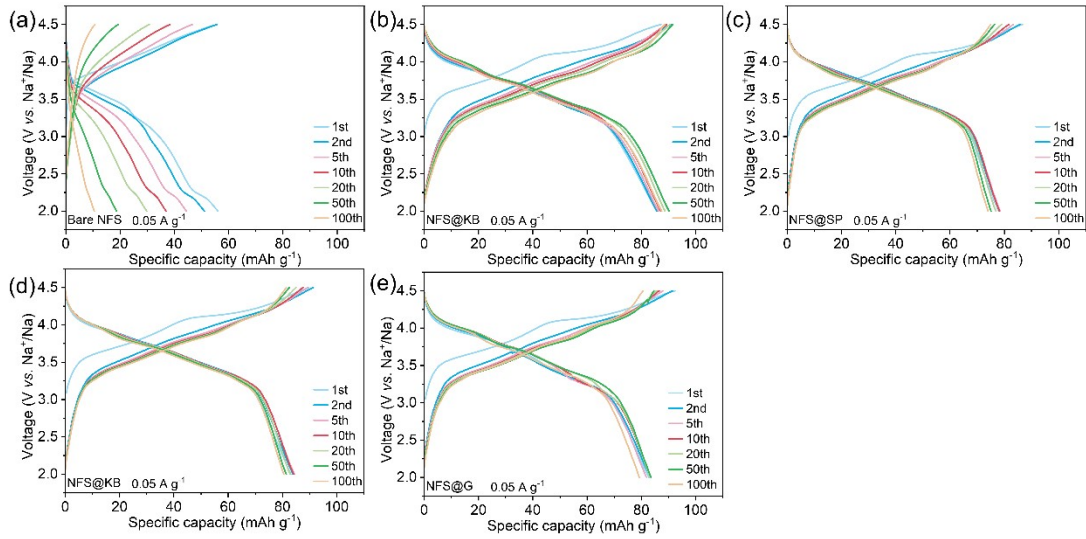
3 mappings of (a) NFS@SP, (b) NFS@AB, and (c) NFS@G.

4



1  
 2 **Figure S7.** (a) Cycling performance at 0.05 A g<sup>-1</sup> and (b) rate performance of  
 3 NFS@KB, bare NFS and NFS ADD KB.

4

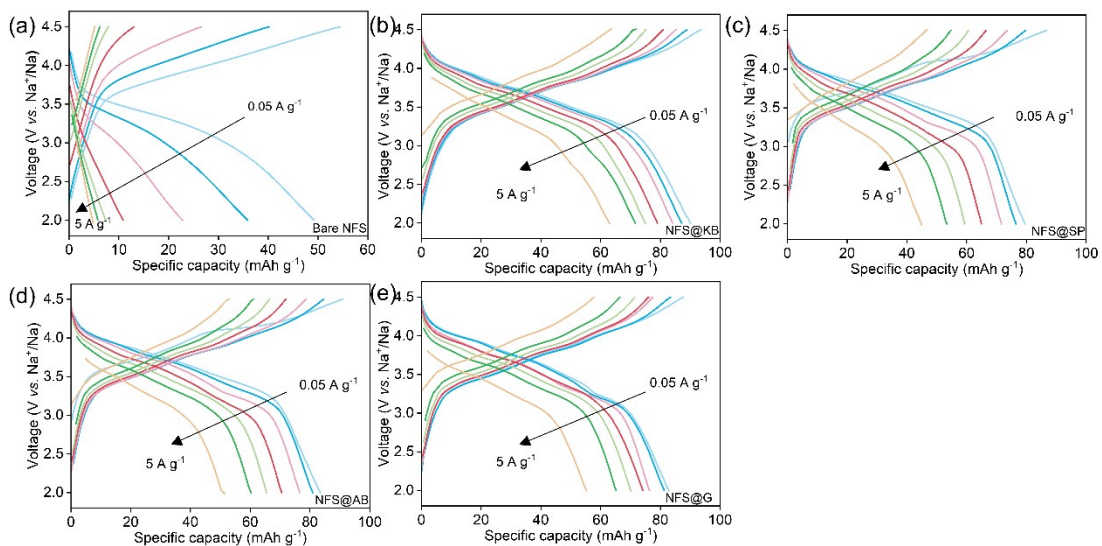


1

2 **Figure S8.** The select charge/discharge curves of (a) Bare NFS, (b) NFS@KB, (c)

3 NFS@SP, (d) NFS@AB, and (e) NFS@G.

4

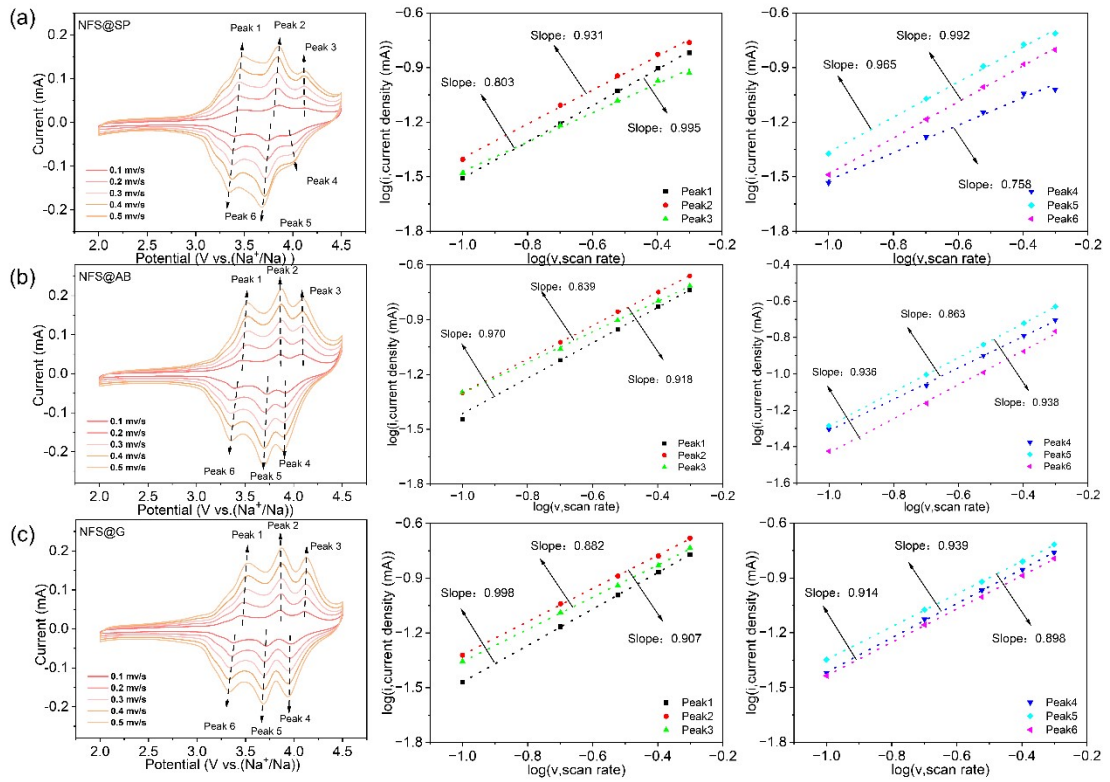


1

2 **Figure S9.** Charge/discharge curves of (a) bare NFS, (b) NFS@KB, (c) NFS@SP, (d)

3 NFS@AB, and (e) NFS@G at different current densities.

4



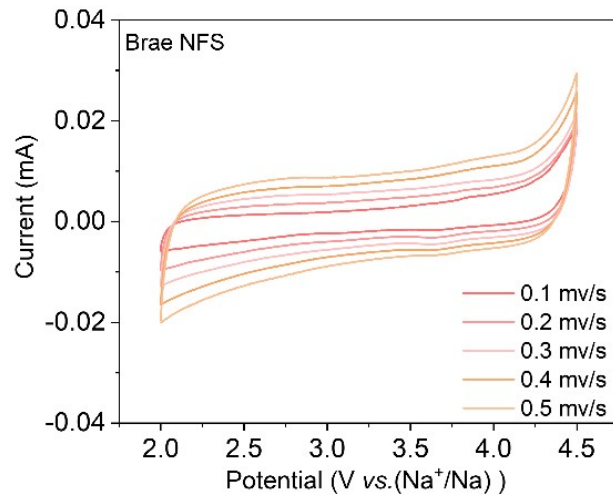
1

2 **Figure S10.** CV curve of NFS@C from 0.1  $\text{mV s}^{-1}$  to 0.5  $\text{mV s}^{-1}$ , The relevant b-values

3 determination for the anodic and cathodic peaks of corresponding (a) NFS@SP, (b)

4 NFS@AB and (c) NFS@G.

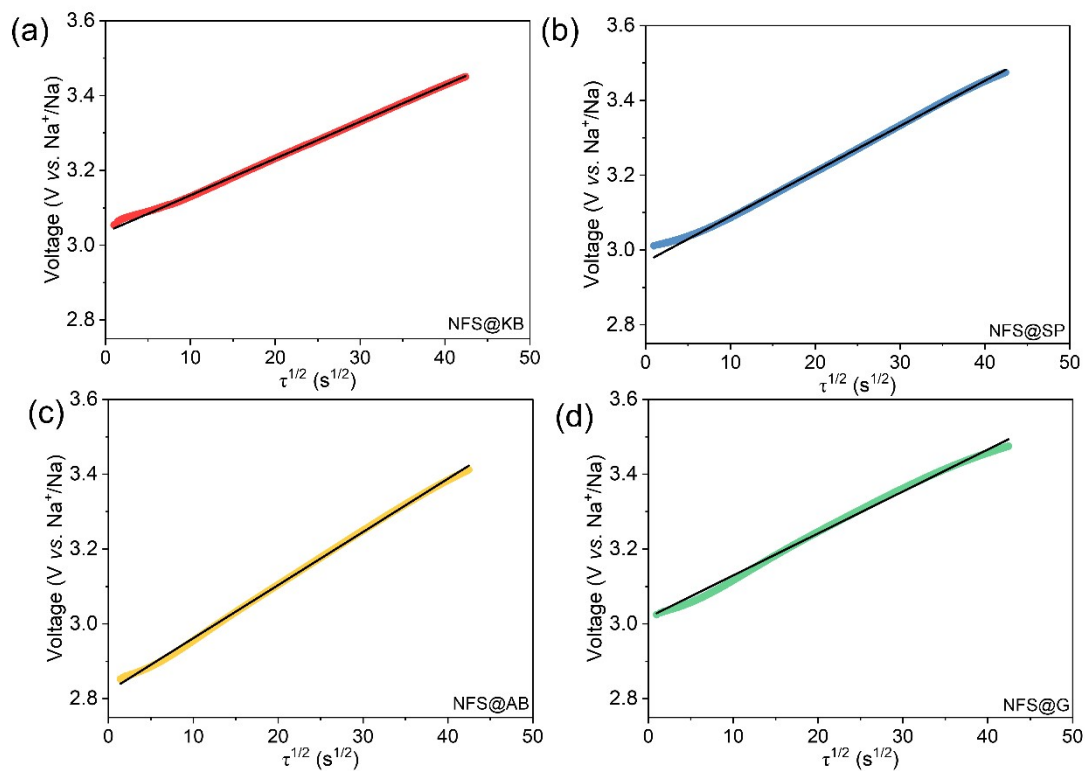
5



1

2 **Figure S11.** CV curve of bare NFS from 0.1 mV s<sup>-1</sup> to 0.5 mV s<sup>-1</sup>.

3

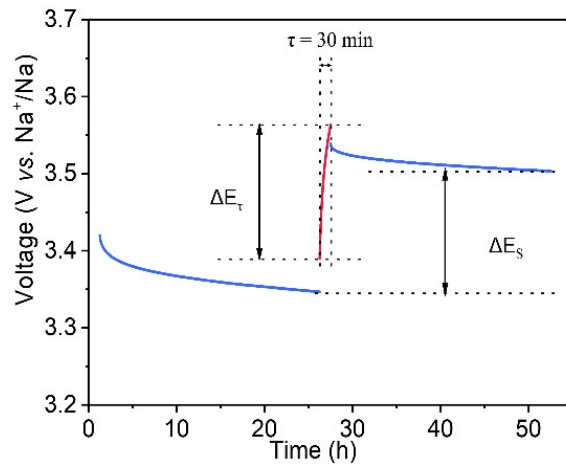


1

2 **Figure S12.** Linear relationship of voltage vs.  $\sqrt{\tau}$  in GITT of (a) NFS@KB, (b)

3 NFS@SP, (c) NFS@AB, and (d) NFS@G.

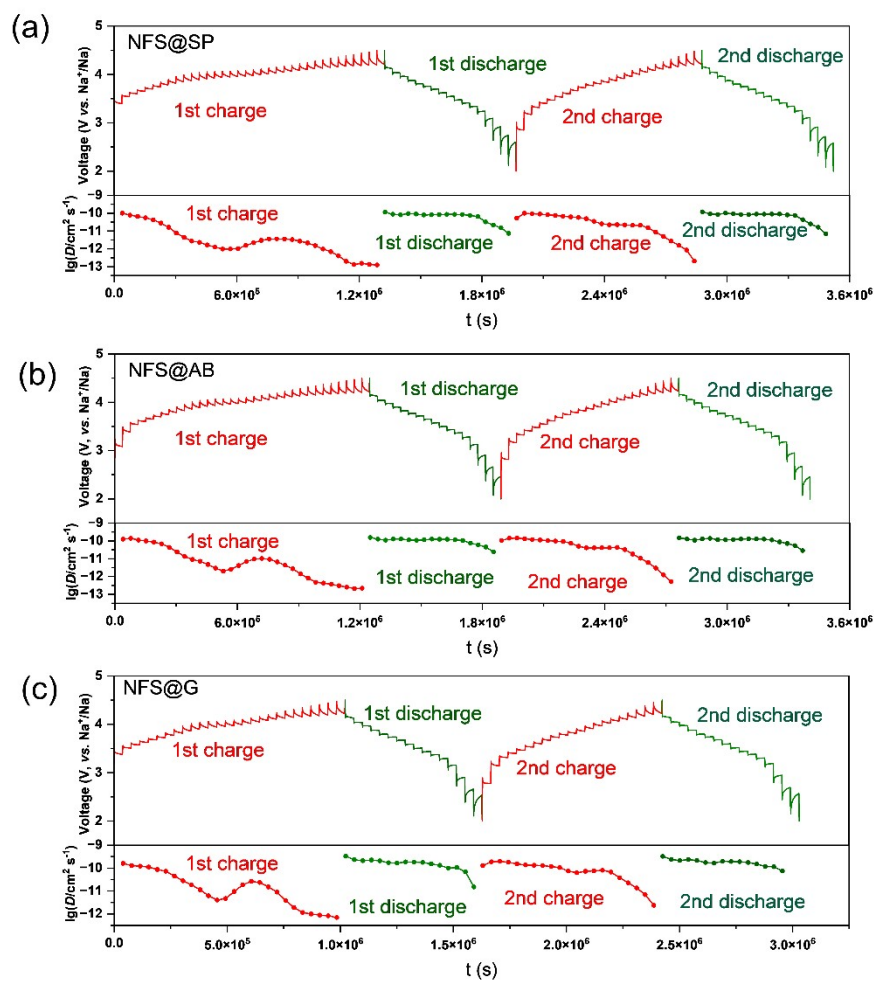
4



1

2 **Figure S13.** The time versus voltage curve for a single titration.

3



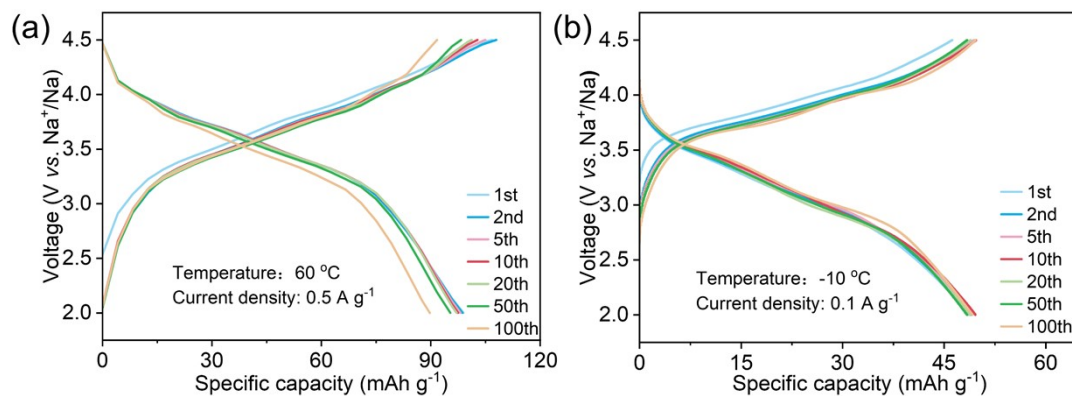
1

2 **Figure S14.** Galvanostatic intermittent titration technique (GITT) curves of (a)

3 NFS@SP, (b) NFS@AB, and (c) NFS@G material for the charge and discharge

4 process.

5

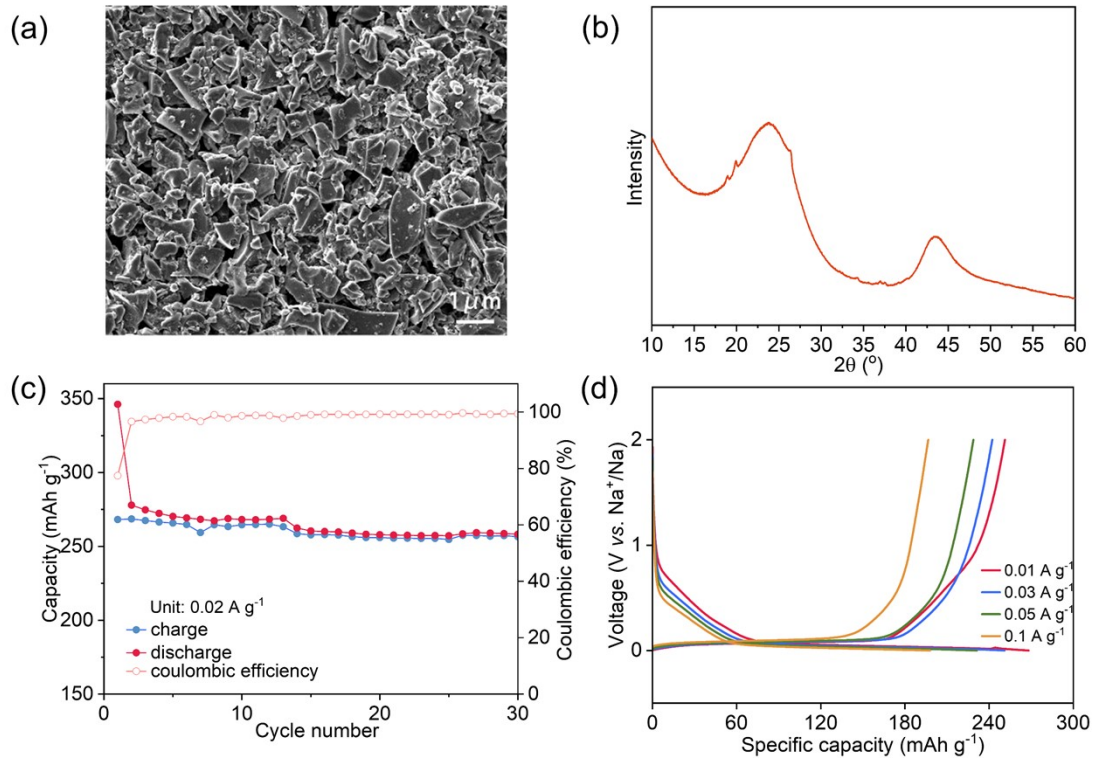


1

2 **Figure S15.** (a) The select charge/discharge curves for NFS@KB at 0.5 A g<sup>-1</sup> at 60 °C,

3 (b) the select charge/discharge curves for NFS@KB at -10 °C at 0.1 A g<sup>-1</sup>.

4



1

2 **Figure S16.** (a) SEM, (b) XRD, (c) cycling properties, and (d) rate performance of

3 commercially available hard carbon.

4

1 **Table S1.** Mass loadings of polyanionic cathode materials in reported literatures.

| Cathode materials   | Active material loading          | Reference |
|---|----------------------------------|-----------|
| $\text{Na}_2\text{FeP}_2\text{O}_7$   | 1.5-3.5 $\text{mg cm}^{-2}$      | 1         |
| $\text{Na}_4\text{Fe}_3(\text{PO}_4)_2(\text{P}_2\text{O}_7)@\text{C}$            | $\sim 2.5 \text{ mg cm}^{-2}$    | 2         |
| $\text{Na}_4\text{Fe}_3(\text{PO}_4)_2(\text{P}_2\text{O}_7)@\text{C}@r\text{GO}$ | $\sim 2.5 \text{ mg cm}^{-2}$    | 2         |
| $\text{Na}_2\text{MnP}_2\text{O}_7$   | $1.6 \pm 0.1 \text{ mg cm}^{-2}$ | 3         |
| $\text{Na}_2\text{Fe}(\text{SO}_4)_2@r\text{GO}/\text{C}$                         | $\sim 1.5 \text{ mg cm}^{-2}$    | 4         |
| $\text{Na}_2\text{Fe}_2(\text{SO}_4)_3@\text{C}$                                  | $\sim 1.6 \text{ mg cm}^{-2}$    | 5         |
| $\text{Na}_2\text{Fe}_2(\text{SO}_4)_3@\text{C}@r\text{GO}$                       | $\sim 1.6 \text{ mg cm}^{-2}$    | 5         |
| $\text{Na}_3\text{V}_2(\text{PO}_4)_3$  | 3.2-3.3 $\text{mg cm}^{-2}$      | 6         |
| $\text{Na}_2\text{Mn}_2(\text{SO}_4)_3$   | $\sim 2.2 \text{ mg cm}^{-2}$    | 7         |
| $\text{NaFePO}_4@\text{C}$  | $\sim 2.5 \text{ mg cm}^{-2}$    | 8         |
| $\text{Na}_2\text{Fe}_2(\text{SO}_4)_3@r\text{KB}$                                | 1.5-2.0 $\text{mg cm}^{-2}$      | This work |

2

3

## 1 References

- 2 1. H. Kim, R. A. Shakoor, C. Park, S. Y. Lim, J.-S. Kim, Y. N. Jo, W. Cho, K.  
3 Miyasaka, R. Kahraman, Y. Jung and J. W. Choi, *Adv. Funct. Mater.*, 2013, **23**,  
4 1147-1155.
- 5 2. J. Gao, Y. Tian, Y. Mei, L. Ni, H. Wang, H. Liu, W. Deng, G. Zou, H. Hou and X.  
6 Ji, *Chem. Eng. J.*, 2023, **458**, 141385.
- 7 3. H. Li, X. Chen, T. Jin, W. Bao, Z. Zhang and L. Jiao, *Energy Stor. Mater.*, 2018,  
8 **16**, 383-390.
- 9 4. G. Yao, X. X. Zhang, Y. L. Yan, J. Y. Zhang, K. M. Song, J. Shi, L. W. Mi, J. Y.  
10 Zheng, X. M. Feng and W. H. Chen , *J Energy chem.*, 2020, **50**, 387-394.
- 11 5. M. Chen, D. Cortie, Z. Hu, H. Jin, S. Wang, Q. Gu, W. Hua, E. Wang, W. Lai, L.  
12 Chen, S. -L. Chou, X. -L. Wang and S. -X. Dou, *Adv. Energy Mater.*, 2018, **8**,  
13 1800944.
- 14 6. Y. Liu, X. Wu, A. Moezz, Z. Peng, Y. Xia, D. Zhao, J. Liu and W. Li, *Adv. Energy*  
15 *Mater.*, 2022, **13**, 2203283.
- 16 7. B. awaz and M. O. Ullah, *J. Mater. Sci.: Mater. Electron.*, 2021, **32**, 14509-14518.
- 17 8. Y. Liu, N. Zhang, F. Wang, X. Liu, L. Jiao and L.-Z. Fan, *Adv. Funct. Mater.*, 2018,  
18 **28**, 1801917.